Flap Position of Free Memapsin 2 (β-Secretase), a Model for Flap Opening in Aspartic Protease Catalysis[†,‡]

Lin Hong[§,||] and Jordan Tang*[,§,#]

Protein Studies Program, Oklahoma Medical Research Foundation, Oklahoma City, Oklahoma 73104, Zapaq Incorporated, Oklahoma City, Oklahoma 73104, and Department of Biochemistry and Molecular Biology, University of Oklahoma Health Science Center, Oklahoma City, Oklahoma 73104

Received January 23, 2004; Revised Manuscript Received February 24, 2004

ABSTRACT: The three-dimensional structure of unbound human memapsin 2 (β-secretase) protease domain determined at 2.0-Å resolution has revealed a new position of the flap region, which appears to be locked in an "open" position. While the structure outside of the flap is essentially the same as the structure of memapsin 2 bound to an inhibitor, the flap positions are 4.5 Å different at the tips. The open position of the flap in the current structure is stabilized by two newly formed intraflap hydrogen bonds and anchored by a new hydrogen bond involving the side chain of Tyr 71 (Tyr 75 in pepsin numbering) in a novel orientation. In molecular modeling experiments, the opening of the flap, 6.5 Å at the narrowest point, permits entrance of substrates into the cleft. The narrowest point of the opening may function to discriminate among substrates based on sequence and shape. The observed flap opening may also serve as a model for the flap movement in the catalytic mechanism of eukaryotic aspartic proteases and provide insight for the side-chain selection in the design of memapsin 2 inhibitors.

The active site of aspartic proteases is characteristically covered over by flaps. In eukaryotic aspartic proteases, a single flap of about 14 residues in a β-hairpin structure covers the center part of the active-site cleft and is perpendicular to the cleft (*1*). In retroviral proteases, two flaps, one from each unit of the homodimer, meet over the central part of the cleft (*2*). In both classes of aspartic proteases, when the active-site cleft is occupied by a substrate, the flaps contribute to hydrolytic specificity. However, during the catalytic cycle, the flaps must open to allow the entrance of the substrates into the catalytic clefts and possibly the release of hydrolytic products. The structural basis for the flap opening remains obscure. Several crystal structures of the unbound eukaryotic aspartic proteases (PDB ID: cathepsin D 1LYB, renin 1BBS, pepsin 1PSN, endothiapepsin 2ER6, yeast proteinase A 1FQ5, and penicillopepsin 1APT) reveal only a small (about 2 Å) difference in flap positions when compared to those in the corresponding structures of enzyme−inhibitor complexes (PDB ID in the same order: 1LYA, 2REN, 4PEP, 1ER8, 1FMU, and 3APP). The openings in these unbound structures are not sufficiently large enough to permit the transport of the substrates and products. In human immunodeficiency virus type 1 (HIV-1) protease, the positions of the flaps in the crystal structures of the unbound and inhibitor-bound enzymes reflect relatively large movement (7 Å at the tips) (*3*). However, in all cases, the flap openings are not sufficiently wide enough for substrate entrance. Thus, the structural basis of flap opening remained unclear.

However, in the eukaryotic aspartic proteases, the mechanism of flap opening is of significance scientifically because many aspartic proteases are intimately involved in human diseases, as exemplified by the involvement of renin in hypertension and HIV protease in AIDS. More recently, memapsin 2 (*4*) (also BACE and ASP-2) (*5*−*8*) has been extensively studied because it was identified as β-secretase that initiates the production of amyloid-β leading to the pathogenesis of Alzheimer's disease (*9*). Thus, memapsin 2 is a primary target in the development of inhibitor drugs for treating Alzheimer's disease. We reported previously that crystallographic structures of human memapsin 2 catalytic unit bound to transition-state inhibitors (*10, 11*). These structures defined the structural template for the inhibitor design. The flap positions in these structures are similar to those observed in other eukaryotic aspartic protease−inhibitor complexes listed above. Basically, the flap tightly covers the inhibitor, and the flap residue Tyr 71 (Tyr 75 in pepsin numbering) contributes to the binding of the side chains of the P_1 and P_2' residues.

We undertook the structural determination of the free memapsin 2 protease domain in order to document the conformational change in this protease because of the binding of strong inhibitors and to further define the structural basis of memapsin 2 catalysis. This information may facilitate the design of new inhibitors. Here, we report that the major structural difference in the bound and unbound memapsin 2 is a large movement of the flap of about 4.5 Å at the tip. The flap in the unbound memapsin 2 appears in a novel "open" position permitting access to the active-site cleft.

[†] This study was supported by National Institute of Health (Grant AG-18933) and Alzheimer's Association Pioneer Award to J.T.

[‡] The atomic coordinates of the free memapsin 2 structure have been deposited in the Protein Data Bank (1SGZ).

* To whom correspondence should be addressed. E-mail: jordan-tang@omrf.ouhsc.edu.

[§] Oklahoma Medical Research Foundation.

[||] Zapaq Inc.

[#] University of Oklahoma Health Science Center.

10.1021/bi0498252 CCC: $27.50
Published on Web 04/01/2004

EXPERIMENTAL PROCEDURES

Protein Purification and Crystallization. Recombinant human promemapsin 2 was produced in *Escherichia coli* as inclusion bodies, refolded by rapid dilution, and purified on a S-300 gel filtration column as previously described (*4*, *10*). Purified promemapsin 2 was activated by clostripain as described by Ermolieff et al. (*12*) with minor modifications followed by purification with anion exchange chromatography (*4*).

Crystals of unbound memapsin 2 were grown using a hanging drop vapor diffusion method as previously described (*10*, *11*) with minor modifications. For the initial screen, 5 μl of purified memapsin 2 at 20 mg/mL were mixed with an equal volume of reservoir solution containing 16−22% PEG[1] 8000 buffered with 0.1 M sodium cacodylate in a pH range of 6.2−7.4. Polymeric crystals unsuitable for X-ray diffraction appeared in a few days at 20% PEG 8000 at pH 7.0 and 20 °C. Further optimizations including variations in protein concentrations, pH values, temperature, and sample−reservoir buffer ratio did not improve the crystal quality significantly. However, no nucleation was observed for PEG concentrations below 16%. Therefore, streak microseeding for these hanging drops preequilibrated for 2 days containing 13−15% PEG 8000 in a pH range of 6.2−7.4 was carried out with the same memapsin 2 concentration at 17 °C using the polymeric crystals and a previously described procedure (*13*). Monoclinic crystals suitable for structure determination resulted after streak seeding at 15% PEG 8000 at pH 6.5 and grow to full size (0.3 × 0.2 × 0.05 mm) in about 3 weeks.

Data Collection and Processing. Memapsin 2 crystal was soaked in the mother liquor plus 20% (v/v) glycerol and quickly frozen under a cryogenic nitrogen gas stream. Diffraction data of a single crystal were recorded on a Mar 345 image plate mounted on a MSC−Rigaku RU-300 X-ray generator with Osmic focusing mirrors. Data were integrated and merged using the DENZO and SCALEPACK (*14*). The initial index with DENZO gave a low distortion index of 0.1 for the primitive monoclinic crystal lattice. This value was significantly higher for crystal forms with higher symmetry. Trial index and integration in higher symmetry forms such as orthorhombic and tetragonal lattices resulted in unacceptable error indexes and unreasonably high R_{merge} values. Therefore, the crystal form was determined to be monoclinic. Systematic absence of reflections suggested the space group to be $P2_1$.

Structure Determination. The structure was determined by molecular replacement implemented with the program AmoRe (*15*) using the previously determined memapsin 2 structure (PDB ID: 1M4H) as a search model. Rotation and translation functions followed by the rigid-body refinement with data from 15- to 3.5-Å resolution in space group $P2_1$ gave unambiguous solutions for the four memapsin 2 molecules in the asymmetric unit with a correlation factor of 72% and an *R* factor of 0.34. Repeating the calculation in space group *P*2 or *C*2 did not give any distinctive solution. To confirm that the space group is $P2_1$, self-rotation and Patterson maps were calculated and no additional crystallographic symmetry was found. Refinement procedures including simulated annealing were carried out with CNS (*16*), and iterative cycles of model building used graphics program O (*17*). A random selection of 8% of reflections was set aside as the test set for cross validation during the refinement. Significant changes were observed within the flap (residues 68−75), and the corresponding structure was rebuilt based on electron density. Continuous and well-defined electron densities were observed for the flap region (residues 65−79, Figure 2) as well as other parts of memapsin 2. Water molecules were located in $|F_o| - |F_c|$ maps contoured at 3 σ level. The four molecules in the crystallographic asymmetric unit have essentially identical structures. The final model has good stereochemistry and statistics (Table 1).

Table 1: Data Collection and Refinement Statistics for Free Memapsin 2

space group	$P2_1$
unit cell a, b, and c (Å)	86.2, 130.8, 88.7
α, β, γ (deg)	90, 97.3, 90
resolution (Å)	50.0−2.0
number of observed reflections	496 038
number of unique reflections	130 359
R_{merge}[a]	0.085
	0.444 (2.07−2.00 Å)
data completeness (%)	99.4 (50.0−2.00 Å)
	98.2 (2.07−2.00 Å)
$I/\sigma(I)$	14.2 (50.0−2.00 Å)
	2.9 (2.07−2.00 Å)
$R_{working}$[b]	0.196
R_{free}[b]	0.228
RMS deviation from ideal values	
bond length (Å)	0.009
bond angle (deg)	1.6
number of water molecules	901
average *B* factors (Å^2)	
protein	25.9
solvent	29.3

[a] $R_{merge} = \sum_{hkl}\sum_i |I_{hkl,i} - \langle I_{hkl}\rangle| / \sum_{hkl}\langle I_{hkl}\rangle$, where $I_{hkl,i}$ is the intensity of the *i*th measurement and $\langle I_{hkl}\rangle$ is the weighted mean of all measurements of I_{hkl}. [b] R_{work} and $R_{free} = \sum||F_o| - |F_c|| / \sum|F_o|$, where F_o and F_c are the observed and calculated structure factors, respectively. Reflections with an $F_o/\sigma(F_o)$ of ≥0.0 are included in the refinement and *R* factor calculation.

RESULTS

Crystal Structure of Free Memapsin 2 Protease Domain. The crystal structure of free human memapsin 2 protease domain was solved in the monoclinic crystal form at the resolution of 2.0 Å. The four molecules in the crystallographic asymmetric unit have virtually identical structures with a 0.76-Å maximum RMS deviation between pairs of the four molecules. The refined free memapsin 2 structure has topological folding identical to the previously solved memapsin 2 structures bound to transition-state inhibitors OM99-2 (*10*) and OM00-3 (*11*). The RMS separation between the unbound and bound (OM00-3) structures is 0.83 Å for all atoms and 0.61 Å for the main-chain atoms. However, as described below, significant structural differences were found in the flap region.

Flap Conformation of Free Memapsin 2. The flap (residues 65−79) in the free memapsin 2 moves significantly away from the substrate-binding cleft (Figure 1a) as compared to its position in the inhibitor-bound enzyme. The main-chain RMS deviation over the tip region of the flap (residues 71−

[1] Abbreviations: PEG, poly(ethylene glycol); RMS, root-mean-square.

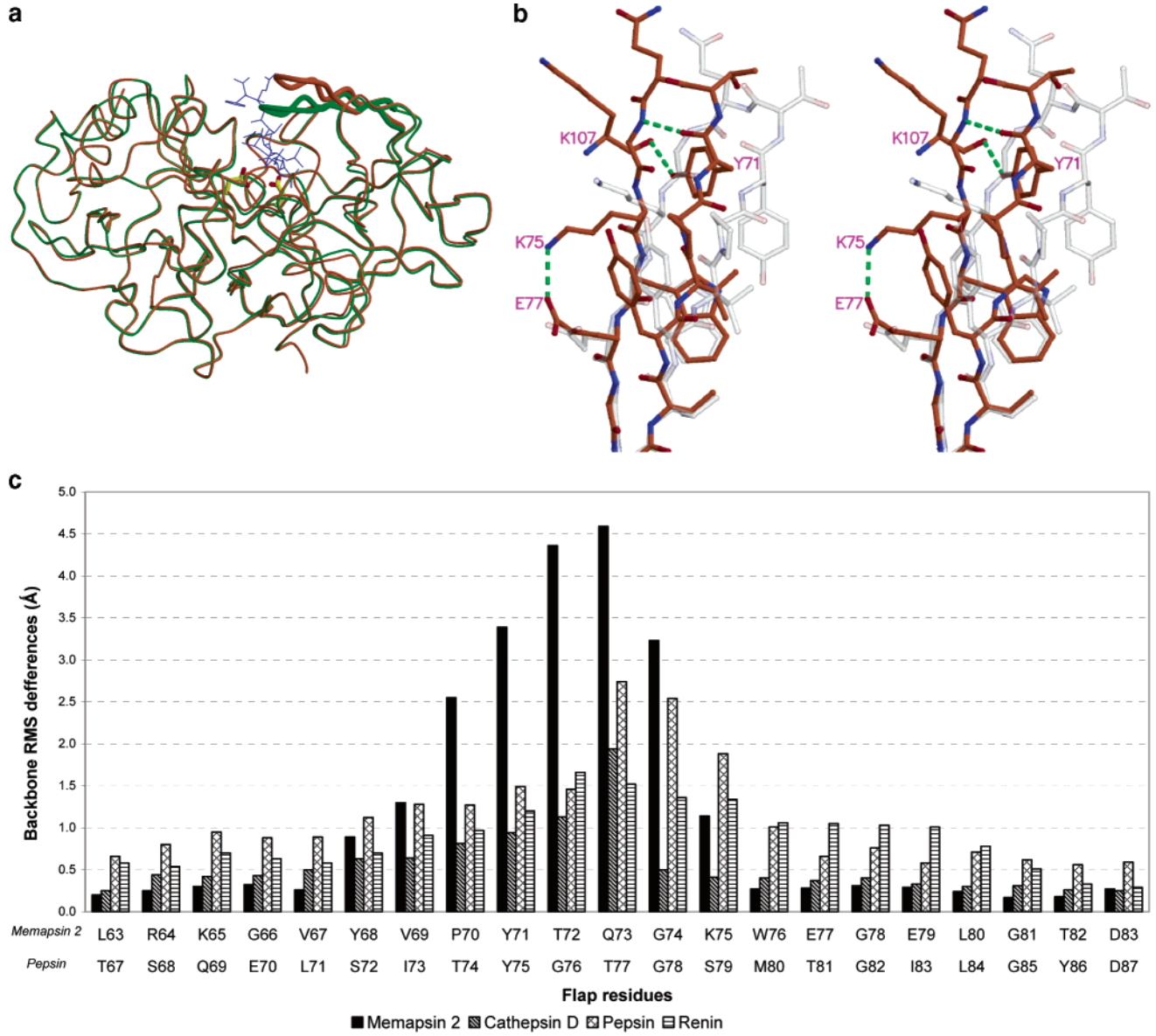

FIGURE 1: (a) Superimposed foldings of free (coral) and inhibitor-bound (green) memapsin 2 protease domain illustrate the difference in flap positions. Two active-site aspartic acids are shown in yellow. Inhibitor (OM00-3) is shown by a blue stick model. Flaps are shown with a thick-thread line. (b) Stereoview of the difference in flap positions of free (coral) and inhibitor-bound memapsin 2 (light gray). Three unique hydrogen bonds in the structure of the free memapsin 2 flap are shown in green dotted lines. Notice the differences between side-chain orientations of Tyr71, Lys75, and Glu77. (c) Positional change of the backbone atoms between the flaps of free and inhibitor-bound human aspartic proteases. The four clustered columns at each residue represent respectively, from left to right, the RMS difference of memapsin 2 (solid bar), human cathepsin D (slashed bar, PDB ID: 1LYB and 1LYA for the bound and unbound enzyme), pepsin (crossed bar, PDB ID: 1PSO and 4PEP), and human renin (horizontal bar, PDB ID: 1HRN and 2REN). The residue numbers on the top line are those of memapsin 2 and on the second line are those of pepsin. The tip of the flap is at T72, Q73 for memapsin 2, and G76, T77 for pepsin.

74) is 3.9 Å between the bound and unbound enzyme. The change of position in the N-terminal strand (residues 65−72) of the flap hairpin involves five residues. While the movement is small at Tyr 68, it increases with each residue to the tip where the displacement at Thr 72 is about 4.4 Å (parts b and c of Figure 1). Only three residues (residues 73−75) moved significantly in the C-terminal strand of the flap. Although Gln 73 has the highest displacement of 4.6 Å, the movement decreases in the next three residues and ends at Lys 75 (Figure 1c).

The flap of free memapsin 2 is in a three-strand β sheet with 12 antiparallel hydrogen bonds (Figure 2). One β-structure hydrogen bond is unique to the free enzyme. Residues Tyr 71 (O) and Gly 74 (N), which are separated by a distance of 4.2 Å in the bound enzyme, form a strong hydrogen bond with a distance of 2.8 Å in free memapsin 2 (Figure 1b). There is a new hydrogen bond containing an ion pair between Lys 75 (NZ) and Glu 77 (OE2) having a bond distance of 2.8 Å compared to the distance of 8.2 Å in the bound enzyme (Figure 1b). Other intraflap hydrogen bonds and those between the C-terminal strand of the flap and the β strand of residues 101−107 are present in both the bound and free enzymes, and their bond distances are not significantly changed. In the free enzyme, the side chain of Tyr 71 adopts a unique orientation to form a new hydrogen bond (distance of 2.8 Å) between its phenolic OH and the backbone carbonyl of residue Lys 107 (Figure 1b). These three new hydrogen bonds should contribute to the stabilization of the three-strand

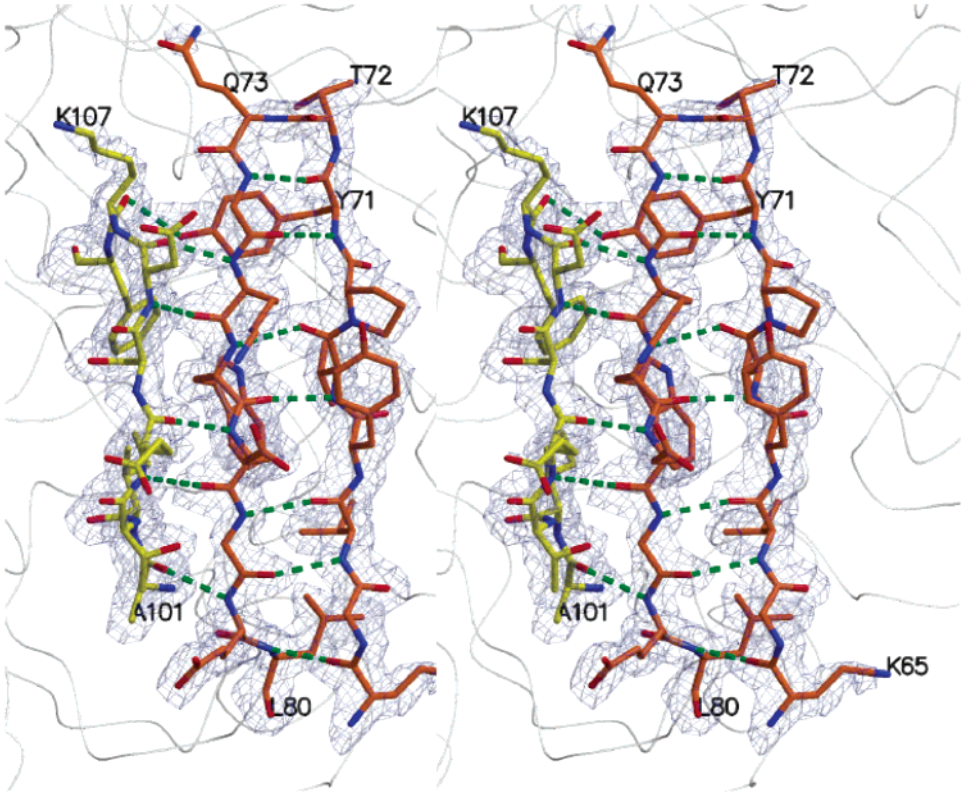

FIGURE 2: Hydrogen bonds (green dotted line) involving flap residues in free memapsin 2. The strands of the memapsin 2 flap are in coral, and the third strand (residues 101−107) is in yellow. Electron density is from the $2F_o - F_c$ map contoured at 1 σ level.

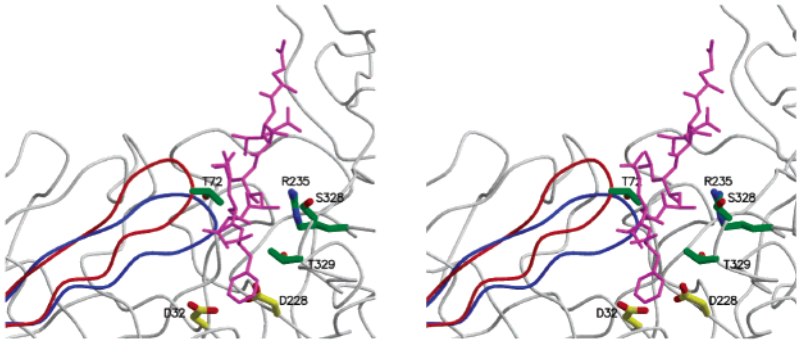

FIGURE 3: Stereo presentation of the opening of the flap in free memapsin 2 (red) and that of the inhibitor-bound enzyme (blue). The side chains of the "bottleneck" residues (green) from both sides of the active-site cleft are shown. Two catalytic aspartyl groups are shown in yellow. In modeling, a transition-state inhibitor OM00-3 (burgundy) was able to transit the bottleneck and enter the cleft. The opening in the bound memapsin 2 structure does not permit the entrance.

β sheet involving the flap and strand 101−107 and the opening of the substrate cleft.

The narrowest point of the flap opening, which is about 6.5 Å, consists of the flap residue Thr 72 at one side of the cleft and residues Arg 235, Ser 328, and Thr 329 on the other side (Figure 3). The conformation of the flap in free memapsin 2 is clearly not influenced by crystal packing. Of the four crystallographically independent molecules in the asymmetric unit, two of them have no crystal contacts in the flap region and the other two have only minor contacts. Yet, the flap conformations are the same in all four molecules.

DISCUSSION

Flap in Free Memapsin 2 Is at an Open Position Anchored by Tyr 71. The observed flap conformation likely represents its open position in the catalytic cycle of memapsin 2. The hydrogen bonds among three antiparallel β strands of the flap in this conformation, including three new ones (Figure 2), have distances and angles near optimal values. Thus, this conformation is an energetically stable form for the free enzyme. The movement of the flap toward the closed conformation, as in the inhibitor-bound enzyme (*10*, *11*), breaks the hydrogen bonds between flap residues Tyr 71 (O) and Gly 74 (N) and residues Lys 75 (NZ) and Glu 77 (OE2), as well as the hydrogen bond involving Tyr 71 (OH) and Lys 107 (O). The resulting destabilization is, however, compensated by the interaction with a substrate or an inhibitor. A flap movement toward an even more open conformation, on the other hand, would result in a stability loss because the hydrogen bonds in the three-strand β sheet would be distorted or stretched out of the optimal positions with little compensatory gain from other interactions. The possibility that the flap can open further by changing the

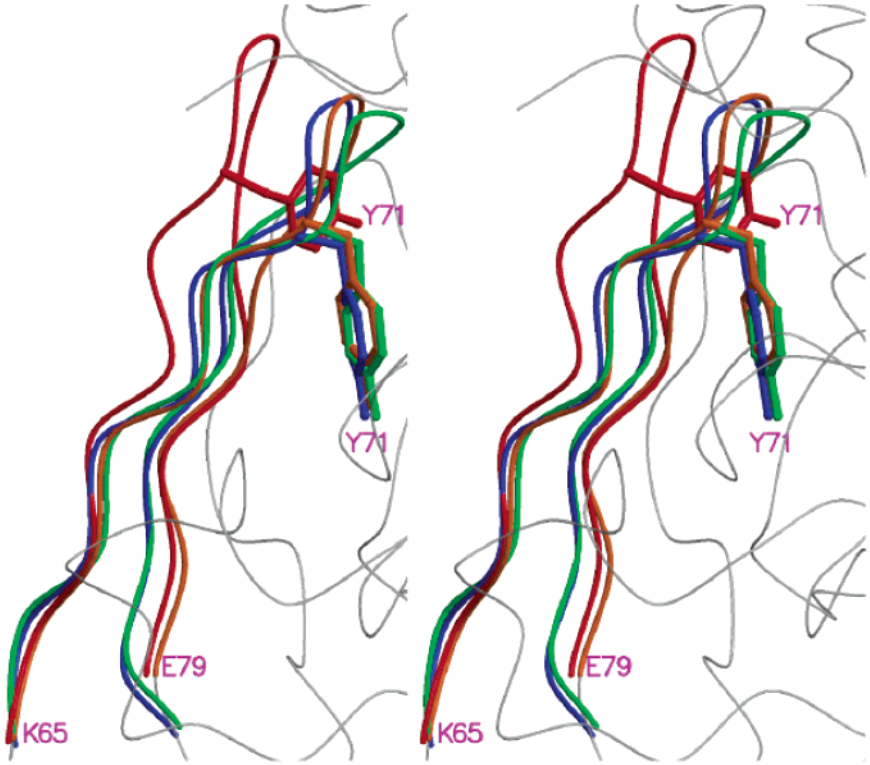

FIGURE 4: Stereo presentation of Tyr 71 positions between free (burgundy) and inhibitor-bound (coral) memapsin 2 and the corresponding Tyr (residue 78) in free (blue) and bound (green) cathepsin D. The positions of this Tyr in free and bound pepsin (residue 75) and renin (residue 83) (not shown) are very near those of cathepsin D.

topological relationships of the two lobes (*18*) is not being considered here. Such a movement would involve a rearrangement of the large interface between the lobes and is not supported by any crystallographic or physical chemical evidence. Together, the above points would argue that the currently observed flap position is the predominant conformation for free memapsin 2 in solution.

Tyr 71 plays a unique role in the open-flap conformation. In the inhibitor bound "closed" flap, the side chain of Tyr 71 makes a hydrogen bond to the indole nitrogen of Trp 76 (bond distance of 3.1 Å) and has contacts with residues located in subsites P_1 and P_2' of the inhibitor. In the free enzyme, not only does Tyr 71 move away from the substrate cleft along with the flap, it forms a new hydrogen bond to backbone carbonyl of Lys 107 (bond distance of 2.8 Å, Figure 1b). Significant changes in side-chain torsion angles occur for Tyr 71 from the free to bound enzyme in which Chi1 and Chi2 values change from +59° and +75° to −58° and −93°, respectively. The main-chain torsion angles at Tyr 71, in which Phi and Psi values are −159.2 and +152.7 for the unbound and −121.0 and +174.0 for the bound enzyme, respectively, make it possible to form the new hydrogen bond between Tyr 71 (O) and Gly 74 (N). In the crystal structures of other free eukaryotic aspartic proteases, the corresponding tyrosines (residue 75 in pepsin numbering) are mostly in the same orientation as in the bound enzymes, exemplified by cathepsin D (Figure 4). Two exceptions have been observed. In free chymosin, the corresponding tyrosine occupies the S_1 pocket (*19*, *20*) in a "self-inhibited" conformation (*21*). This conformation would require an adjacent glycine at position 76 (pepsin numbering) (*22*) that is a threonine in memapsin 2 (Figure 1c). An altered conformaton of this tyrosine also occurs in free proteinase A of *Saccharomyces cerevisiae* (*22*). In all of these free enzymes, however, the flap remains closed. The unique orientation of Tyr 71 with a new hydrogen bond suggests that its side chain may serve as an anchor for the flap at the open position in free memapsin 2.

Implications of Open Flap on the Catalysis and Inhibition of Memapsin 2. Implicit in an open-flap conformation is the accessibility of substrates and inhibitors to the active-site cleft. Using computer modeling, we found that inhibitor OM00-3 (*11*, *23*) can enter the cleft through the opening of the free memapsin 2 structure (Figure 3). OM00-3 is a transition-state analogue of a substrate with a sequence Glu-Leu-Asp-Leu*Ala-Val-Glu-Phe (where the asterisk represents transition-state isostere hydroxyethylene). The constituent amino acid sequence of OM00-3 was selected because it represents the memapsin 2 preferred residues at each subsite. The octapeptide of this sequence is an excellent memapsin 2 substrate (*23*). Therefore, OM00-3 is a good representative of a substrate in this modeling. For OM00-3 to enter the cleft, conformational flexibility must be present in several side chains of both the substrate and enzyme. This is particularly true for the side chains of P_1 Leu from OM00-3 and residues Thr 72, Arg 235, Ser 328, and Thr 329 around the cleft. Together, these residues create the narrowest point, a bottleneck, of the opening. The fact that these side chains need to be rotated to avoid steric clash as OM00-3 is moved into the cleft illustrates that the opening of the cleft is barely adequate for such a process.

An interesting question is why memapsin 2 has not produced a wider opening through evolution for easier access of its substrates. For example, Thr 72, located at the tip of

the flap, does not form significant contact with inhibitors in the bound enzyme and appears to have little structural role (*10*, *11*). The corresponding residue in pepsin, gastricsin, and chymosin (residue 76 in pepsin numbering) is indeed a glycine, which would have produced a wider opening in memapsin 2. It seems probable that Thr 72 and other bottleneck residues are selected for a function. An intriguing hypothesis results from the fact that memapsin 2 is a membrane-anchored protease and the substrates of memapsin 2 are also membrane-based proteins, such as the amyloid precursor protein. The conformational freedom of the substrate strands near the cleavage sites may be limited by the overall conformation of the protein substrates. Therefore, the involved substrate strands, a minimum of eight residues each, are presented to memapsin 2 in restricted conformations. The bottleneck residues could then serve to select the correct substrates before they are bound to the active site. Such a system would be more efficient with less error than that of free access to the active site, especially in view that memapsin 2 has a broad specificity (*23*). In short, the hypothesis predicts that the narrowness of the opening produces better specificity toward the protein substrate of memapsin 2. Consistent with this hypothesis is the observation that large side chains of Leu, Phe, and Tyr are relatively disfavored at P_1' (*23*) even though a large binding site is present at S_1' of the enzyme (*10*). In our modeling, the P_1' residue must enter the cleft near the bottleneck region (Figure 3), which may account for the fact that the docking of a P_1' Ala is easier than the larger residues. All of these points may have implications on the design of memapsin 2 inhibitor drugs. Even though the conformational freedom of a small-molecular inhibitor will be high, the size of the P_1' side chain may indeed influence the on and off rates and, in turn, the inhibition constants. In addition, inhibitors with locked-in conformation may be desirable for both binding and entrance.

Memapsin 2 as a Model of Flap Opening in Eukaryotic Aspartic Proteases. Comparing flap conformations of eukaryotic aspartic proteases suggests that the structural basis of memapsin 2 flap opening is partially present in others. The open position of the flap is not as energetically favorable in other enzymes as in free memapsin 2. The number of hydrogen bonds between the flap and the third strand are fewer in other aspartic proteases, usually four as compared to six in free memapsin 2. The third strands are shorter in these enzymes, so the anchoring hydrogen bond to the Tyr 75 (pepsin numbering) side chain is not possible. Also, the hydrogen bond between the Lys 75 and Glu 77 side chains is not possible in other aspartic proteases because of the differences in the side chains. All of these factors may contribute to the closed flaps in the crystal structures of the other free enzymes. On the other hand, in contrast to the improved hydrogen-bond pattern within the flap of free memapsin 2, the corresponding bonds are not of optimal length in the free enzymes of other eukaryotic aspartic proteases. For example, free cathepsin D (PDB ID: 1LYA) has an average intraflap hydrogen bond length of 3.06 Å, while the corresponding average bond length is 2.87 Å for free memapsin 2. In other eukaryotic aspartic proteases, the flap must also open to allow the substrate access to the catalytic cleft and the improvements of the flap hydrogen bonds seen in memapsin 2 may indeed be the driving force for an open conformation of the flap in these enzymes at least for a fraction of time. Even though such conformation may not be as prevalent as in free memapsin 2, it can take place in the catalytic cycle of other eukaryotic aspartic proteases for the following reasons. In some of these enzymes, as discussed above, the bottleneck residue 76 (pepsin numbering) is a glycine, which would produce a larger opening and easier access to the active-site cleft. In addition, the conserved flap residue Tyr 75 (pepsin numbering) has been proposed to hydrophobically interact with the P_1 side chain as the initial "capturing step" of the substrate (*24*) in most of the eukaryotic aspartic proteases that prefer a large hydrophobic side chain at P_1. Such a capturing step would be like "a foot in the door" even if the flap opens transiently. Consistent with this mechanism is the fact that Tyr 75 in these enzymes is not hydrogen-bonded as in memapsin 2 and should have more freedom to interact with the substrate at an early stage of the catalytic cycle. Because the S_1 subsite of memapsin 2 prefers to accommodate a smaller side chain such as leucine (*23*), a less-restricted Tyr 71 (Tyr 75 in pepsin numbering) would capture larger residues such as Trp or Tyr more efficiently, which is incompatible with its P_1 specificity. This may be another reason for memapsin 2 to adopt an anchored Tyr 71 conformation and a relatively open flap.

ACKNOWLEDGMENT

The authors thank Drs. A. Wlodawer, J. A. Hartsuck, and G. Koelsch for critical reading of this paper and J. Yohannan, V. Weerasena, and G. Koelsch for memapsin 2 preparation.

REFERENCES

1. Davies, D. R. (1990) The structure and function of the aspartic proteinases, *Annu. Rev. Biophys. Biophys. Chem. 19*, 189−215.
2. Rao, J. K., Erickson, J. W., and Wlodawer, A. (1991) Structural and evolutionary relationships between retroviral and eucaryotic aspartic proteinases, *Biochemistry 30*, 4663−4671.
3. Wlodawer, A., and Gustchina, A. (2000) Structural and biochemical studies of retroviral proteases, *Biochim. Biophys. Acta 1477*, 16−34.
4. Lin, X., Koelsch, G., Wu, S., Downs, D., Dashti, A., and Tang, J. (2000) Human aspartic protease memapsin 2 cleaves the β-secretase site of β-amyloid precursor protein, *Proc. Natl. Acad. Sci. U.S.A. 97*, 1456−1460.
5. Vassar, R., Bennett, B. D., Babu-Khan, S., Kahn, S., Mendiaz, E. A., Denis, P., Teplow, D. B., Ross, S., Amarante, P., Loeloff, R., Luo, Y., Fisher, S., Fuller, J., Edenson, S., Lile, J., Jarosinski, M. A., Biere, A. L., Curran, E., Burgess, T., Louis, J. C., Collins, F., Treanor, J., Rogers, G., and Citron, M. (1999) β-secretase cleavage of Alzheimer's amyloid precursor protein by the transmembrane aspartic protease BACE, *Science 286*, 735−741.
6. Hussain, I., Powell, D., Howlett, D. R., Tew, D. G., Meek, T. D., Chapman, C., Gloger, I. S., Murphy, K. E., Southan, C. D., Ryan, D. M., Smith, T. S., Simmons, D. L., Walsh, F. S., Dingwall, C., and Christie, G. (1999) Identification of a novel aspartic protease (Asp 2) as β-secretase, *Mol. Cell. Neurosci. 14*, 419−427.
7. Yan, R., Bienkowski, M. J., Shuck, M. E., Miao, H., Tory, M. C., Pauley, A. M., Brashier, J. R., Stratman, N. C., Mathews, W. R., Buhl, A. E., Carter, D. B., Tomasselli, A. G., Parodi, L. A., Heinrikson, R. L., and Gurney, M. E. (1999) Membrane-anchored aspartyl protease with Alzheimer's disease β-secretase activity, *Nature 402*, 533−537.
8. Sinha, S., Anderson, J. P., Barbour, R., Basi, G. S., Caccavello, R., Davis, D., Doan, M., Dovey, H. F., Frigon, N., Hong, J., Jacobson-Croak, K., Jewett, N., Keim, P., Knops, J., Lieberburg, I., Power, M., Tan, H., Tatsuno, G., Tung, J., Schenk, D., Seubert, P., Suomensaari, S. M., Wang, S., Walker, D., John, V., et al. (1999) Purification and cloning of amyloid precursor protein β-secretase from human brain, *Nature 402*, 537−540.

9. Selkoe, D. J., and Schenk, D. (2003) Alzheimer's disease: molecular understanding predicts amyloid-based therapeutics, *Annu. Rev. Pharmacol. Toxicol. 43*, 545−584.
10. Hong, L., Koelsch, G., Lin, X., Wu, S., Terzyan, S., Ghosh, A. K., Zhang, X. C., and Tang, J. (2000) Structure of the protease domain of memapsin 2 (β-secretase) complexed with inhibitor, *Science 290*, 150−153.
11. Hong, L., Turner, R. T., III, Koelsch, G., Shin, D., Ghosh, A. K., and Tang, J. (2002) Crystal structure of memapsin 2 (β-secretase) in complex with an inhibitor OM00-3, *Biochemistry 41*, 10963−10967.
12. Ermolieff, J., Loy, J. A., Koelsch, G., and Tang, J. (2000) Proteolytic activation of recombinant promemapsin 2 (pro-β-secretase) studied with new fluorogenic substrates, *Biochemistry 39*, 12450−12456.
13. Ducruix, A., and Giege, R., Eds. (1992) in *Crystallization of Nucleic Acids and Proteins*, pp 112−113, Oxford University Press, New York.
14. Otwinowski, Z., and Minor, W. (1997) Processing of X-ray Diffraction Data Collected in Oscillation Mode, *Methods Enzymol. 276*, 307−326.
15. Navaza, J. (2001) Implementation of molecular replacement in AMoRe, *Acta Crystallogr., Sect. D 57*, 1367−1372.
16. Brunger, A. T., Adams, P. D., Clore, G. M., DeLano, W. L., Gros, P., Grosse-Kunstleve, R. W., Jiang, J. S., Kuszewski, J., Nilges, M., Pannu, N. S., Read, R. J., Rice, L. M., Simonson, T., and Warren, G. L. (1998) Crystallography & NMR system: A new software suite for macromolecular structure determination, *Acta Crystallogr., Sect. D 54*, 905−921.
17. Jones, T. A., Zou, J. Y., Cowan, S. W., and Kjeldgaard (1991) Improved methods for binding protein models in electron density maps and the location of errors in these models, *Acta Crystallogr., Sect. A 47*, 110−119.
18. Tang, J., James, M. N., Hsu, I. N., Jenkins, J. A., and Blundell, T. L. (1978) Structural evidence for gene duplication in the evolution of the acid proteases, *Nature 271*, 618−621.
19. Gilliland, G. L., Winborne, E. L., Nachman, J., and Wlodawer, A. (1990) The three-dimensional structure of recombinant bovine chymosin at 2.3 Å resolution, *Proteins 8*, 82−101.
20. Newman, M., Safro, M., Frazao, C., Khan, G., Zdanov, A., Tickle, I. J., Blundell, T. L., and Andreeva, N. (1991) X-ray analyses of aspartic proteinases. IV. Structure and refinement at 2.2 Å resolution of bovine chymosin, *J. Mol. Biol. 221*, 1295−1309.
21. Andreeva, N., Dill, J., and Gilliland, G. L. (1992) Can enzymes adopt a self-inhibited form? Results of X-ray crystallographic studies of chymosin, *Biochem. Biophys. Res. Commun. 184*, 1074−1081.
22. Gustchina, A., Li, M., Phylip, L. H., Lees, W. E., Kay, J., and Wlodawer, A. (2002) An unusual orientation for Tyr75 in the active site of the aspartic proteinase from *Saccharomyces cerevisiae*, *Biochem. Biophys. Res. Commun. 295*, 1020−1026.
23. Turner, R. T., III, Koelsch, G., Hong, L., Castanheira, P., Ermolieff, J., Ghosh, A. K., Tang, J., Castenheira, P., and Ghosh, A. (2001) Subsite specificity of memapsin 2 (β-secretase): implications for inhibitor design, *Biochemistry 40*, 10001−10006.
24. Tang, J., and Koelsch, G. (1995) A Possible Function of the Flaps of Aspartic Proteases: The Capture of Substrate Side Chains Determines the Specificity of Cleavage Positions, *Protein Pept. Lett. 2*, 257−266.

BI0498252